RSC Advances

PAPER

View Article Online
View Journal | View Issue

Cite this: *RSC Adv.*, 2025, **15**, 24058

Fe and Zn citrate nanoparticles: effect on soil enzyme activities and microbiome†

K. S. V. Poorna Chandrika,*[ab] R. D. Prasad,[c] Anupama Singh[d] and Balaji Gopalan *[a]

Received 28th April 2025
Accepted 20th June 2025

DOI: 10.1039/d5ra02986d

rsc.li/rsc-advances

Iron and zinc citrate nanoparticles (NCs) were developed and evaluated as potential soil-applied plant nutrients. This study investigates the effects of seven synthesized NC formulations—comprising individual and combined Fe and Zn citrate compositions—on soil enzymatic activity and microbial diversity. The impact of NCs was assessed across three concentrations (250, 500, and 1000 mg kg^{-1} of soil) and three incubation periods (30, 60, and 90 days), and was compared to commercial Fe and Zn sources, including salts, chelates, and nano-oxides. Enzyme activities measured included dehydrogenase, urease, acid phosphatase, and alkaline phosphatase. Culture-based microbiological assays were used to quantify fungi, bacteria, and actinomycetes. The results revealed that NCs generally stimulated enzyme activity and microbial populations, particularly at concentrations ≤500 mg kg^{-1}. While slight inhibition was observed at 1000 mg kg^{-1} in some treatments, these effects diminished over time. Strong correlations were found between microbial abundance and enzymatic responses, particularly for dehydrogenase and urease. These findings demonstrate that citrate-stabilized Fe and Zn nanoparticles exhibit low toxicity, support microbial-mediated nutrient cycling, and represent a biosafe alternative to conventional micronutrient sources for soil application.

1. Introduction

With the global population on the rise and soil fertility declining, there's an urgent need for nutrient enrichment to enhance agricultural productivity and mitigate nutrient losses. Nanoparticles have gained attention for their unique characteristics, leading to their widespread application across various agricultural and industrial sectors.[1,2] Their small size and increased reactivity compared to bulk particles make them particularly desirable. However, their growing usage raises concerns about environmental impacts, with studies indicating potential damage to organisms at the DNA level.[3]

Current research focuses on understanding the effects of nanoparticles on soil, encompassing their mobility, leaching, and interactions with soil organisms.[4–6] Soil biological status is a fundamental parameter for assessing the impact of nanoparticles, with studies often concentrating on microbial quantification and biomass as indicators of soil quality.[7–12] Specifically, Ghafari and Razmjoo[13] studied the effect of various iron sources, including oxides, chelate and sulfate. The authors concluded the performance of nano iron oxide is better than other sources in terms of dose.

Several factors are responsible for affecting enzymatic activity.[14–17] The factors that played a pivotal role in the current study are the concentration of nutrients, incubation period, and source and kind of nutrient, which resulted in the diversification of enzymatic activity. Soil enzymes such as dehydrogenase, urease, and phosphatases play vital roles in soil biochemical processes, and disturbances in their activity can disrupt nutrient cycles and plant productivity.[14,15] Recent studies have investigated the effects of various nanoparticles, including carbon nanotubes, silica nanoparticles, and metal oxides, on soil enzymatic activity, revealing both beneficial and adverse effects.[4,18–21] Moreover, soil properties influence nanoparticles' behavior and their subsequent effects on soil enzymes.[6,16,22,23] Environmental concerns are more due to the transfer and contamination of nanoparticles either directly or indirectly which depends on the concentration.[24,25] For instance, Fe_2O_3 nanoparticles with dose of <20 mg L^{-1} was used and was found to promote the increase in the protein levels in *Scenedesmus obliquus*.[26,27] Although bulk Fe_2O_3 is considered inert in soils, its nanoparticle form has been reported to reduce bacterial abundance due to increased reactivity and surface area.[28] To comprehensively assess both beneficial and potentially adverse effects, a higher concentration of 1000 mg kg^{-1} was also tested

[a]*Department of Chemistry, Birla Institute of Technology and Science (BITS) Pilani, Hyderabad Campus, Jawahar Nagar, Kapra Mandal, Hyderabad, 500078, India. E-mail: gbalaji@hyderabad.bits-pilani.ac.in*

[b]*Crop Production Section, ICAR-Indian Institute of Oilseeds Research, Rajendranagar, Hyderabad, 500030, India. E-mail: chandrikahoneychandrika@gmail.com*

[c]*Crop Protection Section, ICAR-Indian Institute of Oilseeds Research, Rajendranagar, Hyderabad, 500030, India*

[d]*Division of Agricultural Chemicals, ICAR-Indian Agricultural Research Institute, Pusa Campus, New Delhi, 110012, India*

† Electronic supplementary information (ESI) available. See DOI: https://doi.org/10.1039/d5ra02986d

under controlled conditions. This approach is commonly used to identify safe exposure thresholds, and the outcomes can inform risk evaluation prior to field application. Nanoforms of iron oxides have been reported to inhibit both Gram-positive and Gram-negative bacteria upon contact with their surfaces.[29] Excessive application of Fe_3O_4 nanoparticles can negatively affect plant development by reducing chlorophyll levels and causing brown patches and stress symptoms.[30] In soil applications, the typical dosage is few hundreds of mg per kg of soil.

Moreover, soil properties significantly influence the behavior of nanoparticles and their subsequent effects on soil enzymatic activities.[6,16,22,23] Environmental concerns largely stem from the potential for nanoparticles to transfer and contaminate ecosystems through both direct and indirect pathways.[24,25] In our previous studies, we synthesized novel Fe and Zn nanocitrates—chelated nutrient formulations—which were evaluated for their effectiveness in enhancing plant nutrient uptake.[31,32] Unlike earlier research that primarily focused on the environmental toxicity and soil interactions of metal and metal oxide nanoparticles (*e.g.*, Fe_2O_3, ZnO), the current study explores a new category of nutrient delivery systems based on citrate-chelated Fe and Zn nanoparticles. These nanocitrates, synthesized *via* ligand-assisted methods and verified through Mössbauer spectroscopy to lack crystalline oxide phases, demonstrate distinctive behavior in soil environments compared to oxide-based nanoparticles. Their chemical composition enhances water solubility, minimizes surface reactivity, and may reduce aggregation and long-term persistence in soil. This innovative approach shifts the emphasis from conventional toxicity assessments to a broader biosafety evaluation, particularly focusing on their effects on soil enzymatic functions and microbial dynamics. By comparing these ligand-stabilized nanonutrients to conventional nutrient sources—including metal salts, EDTA chelates, and commercial nano-oxides—this study provides a unique perspective on their compatibility and environmental impact under realistic soil conditions. Furthermore, we investigated the behavior of citrate nanoparticles following soil application, acknowledging their potential interactions with soil components and influence on biological quality. This work extends our previous findings by systematically evaluating the effects of various citrate nanoparticle formulations on key soil enzymes—dehydrogenase, urease, acid phosphatase, and alkaline phosphatase—alongside commercial controls. Through this, we aim to understand how different nanoparticle concentrations and soil contact durations, representative of typical crop cycles, influence soil enzymatic activity, offering valuable insights into their environmental and agricultural relevance.

2. Materials and methods

2.1. Nanoparticles

Fe and Zn citrate nanoparticles, both individually and in combined compositions totaling seven variants, were synthesized and optimized for performance through principal component analysis in the previous studies. The synthesis procedure and physico-chemical characterization details have been given.[31–33] Here, we report the Mössbauer spectroscopy data to ascertain that the Fe is present in chelate form and not amorphous Fe_2O_3 phase. ^{57}Fe Mössbauer measurements were carried out in transmission mode with ^{57}Co radioactive source in constant acceleration mode using standard PC-based Mössbauer spectrometer equipped with Wissel velocity drive. Velocity calibration of the spectrometer is done with natural iron absorber at room temperature. The spectra were analyzed with NORMOS program. These nanoparticles were subsequently employed to assess their effects on soil enzymatic activity and microbiome diversity. An untreated sample served as a control, while commercial samples containing Fe and Zn were also examined for comparison. The primary objective of this study was to evaluate the impact of synthesized Fe and Zn citrate nanoparticles on soil biological indicators, specifically soil enzyme activities and microbial populations, which are commonly used to assess soil biological health. The composition of the citrate nanoparticles used in the study is provided in Table 1. The metal citrates were prepared following the methodology outlined in previous studies.[31,32] Briefly, nanocitrates were synthesized using a solid-state grinding technique followed by ball milling. The characterization information performed in earlier studies on citrate nanoparticles have been explained (ESI S1†) in chronological order. Besides, we present small-angle X-ray scattering (SAXS) data to deduce the particle size and size distribution for BFC(1 : 1)-6 sample (Fig. S1 and S2†). Specifically, the best-performing samples from prior research were selected for inclusion in this study. These included ball-milled ferric citrate (BFC) at a 1 : 1 ratio (designated as BFC(1 : 1)-6), ball-milled zinc citrate (BZC) at a 1 : 3 ratio (designated as BZC(1 : 3)-6), and various combinations of ferric and zinc citrates denoted as BFZ, with different weight ratios (4 : 6, 5 : 5, 8 : 2), along with ball-milling durations ranging from 2 to 10 hours (BFZ(x : y)-2, -4, -6, -8, -10). The formulations labeled T3 to T7 in Table 1 represent combined Fe/Zn citrate nanoparticles synthesized with varying Fe : Zn weight ratios and ball milling durations. These specific x : y ratios were not arbitrarily chosen, but rather strategically selected based on a previous principal component analysis (PCA)-based performance screening conducted in our earlier studies.[31,32] The screening evaluated a wide matrix of metal-to-citrate ratios and Fe/Zn combinations for their solubility, nutrient release profiles, particle stability, and efficacy (*e.g.*, uptake efficiency, plant response). The selected ratios (*e.g.*, 4 : 6, 5 : 5, 8 : 2) were identified as high-performing combinations that balanced both nutrient bioavailability and particle stability. For instance, the 5 : 5 ratio was found optimal for uniform micronutrient delivery, while 4 : 6 and 8 : 2 represented Zn- and Fe-dominant blends, respectively, to explore nutrient-specific enzymatic effects. The milling durations (2–10 hours) were optimized to achieve suitable particle size and dispersibility. By narrowing down to these top-performing combinations, the study focused on formulations with maximum field relevance and mechanistic insight, rather than exhaustively testing all possible compositions.

Table 1 Sample composition of Fe and Zn sources used in the study

Code	Common name	Treatment	Category
T1	Individual citrates	BFC(1 : 1)-6	Individual citrates
T2		BZC(1 : 3)-6	
T3	Combined citrates	BFZ(4 : 6)-8	Combined citrates
T4		BFZ(5 : 5)-2	
T5		BFZ(5 : 5)-6	
T6		BFZ(8 : 2)-4	
T7		BFCZ(1 : 1 : 1)-6	
T8		$FeSO_4$	Commercial nutrients
T9		$ZnSO_4$	
T10	Geolife	Nano Fe	
T11		Nano Zn	
T12	Fe Gro	Chelated-Fe (Fe-EDTA)	
T13	Zingap	Chelated-Zn (Zn-EDTA)	
T14		Untreated	

The prefix "B" signifies ball-milled samples. Individual ball-milled citrates were coded as BFC(1 : 1) and BZC(1 : 3), with the ratio indicating the mole ratio of metal to citric acid in each sample. For combined citrates, the sample codes were designated as BFZ(x : y), where x and y represent the weight ratios of ferric citrate (FC) and zinc citrate (ZC) used in synthesis, respectively. The number at the end of each sample code corresponds to the duration of ball milling in hours. In addition to the synthesized citrates, commercial nutrients such as $FeSO_4$, $ZnSO_4$, chelated-Fe (Fe-EDTA), chelated-Zn (Zn-EDTA), nano-Fe (Geolife®), and nano-Zn (Geolife®) were procured for comparative purposes in this study. The commercial nanosources, nano-Fe and nano-Zn (Geolife®), were obtained as powders. According to manufacturer specifications, the average particle size of both nanoparticles was reported to be below 100 nm, with purity exceeding 95% (metal content basis). However, independent validation of particle size or surface characteristics was not performed in this study. The nanoparticles are stabilized using undisclosed proprietary dispersants to maintain colloidal stability. These products were used directly as per label dosage (250 mg kg^{-1} of soil) for comparative assessment with synthesized citrate nanoparticles.

The methodology involved assessing soil enzymatic activity and microbiome diversity following the application of the synthesized nanoparticles. Comparisons were made with untreated soil samples and commercial Fe and Zn samples. Through this comprehensive approach, the study aimed to ascertain the effects of the synthesized nanoparticles on soil biological processes, thereby contributing to a better understanding of their potential impact on soil health and productivity.

2.2. Soil characterisation

The soil selected for this study was characterized by its physiochemical properties, as outlined in Table 2. Samples were gathered from a depth of 0–20 cm in the Sangareddy region, known for its arable land, located in Telangana, India. Prior to sampling, precautions were taken to ensure the soil remained free from chemical contamination originating from industrial or urban sources. Immediately after collection, representative soil samples were stored at 4 °C to preserve their freshness for subsequent enzymatic analysis. Before subjecting the soil to treatments and enzymatic assays, it underwent a series of preparations. This included sieving to a particle size of 2 mm, air drying at room temperature, and analysis of its physicochemical properties. The dry weight of the soil was determined by exposing it to 105 °C until a constant weight was achieved. Potentiometric pH measurements were conducted using a 1 M KCl solution with a liquid-to-solid ratio of 2.5 after 24 hours. Soil analysis methods, following the procedures outlined by van Reeuwijk,[34] were employed to determine parameters such as cation exchange capacity (CEC) determined using ammonium acetate at pH 7.0, as well as the levels of phosphorus, potassium, and calcium. Total organic carbon (TOC) was assessed using the Walkley–Black method, which involves chromic acid under wet oxidation conditions. It is important to note that the Walkley–Black method estimates oxidizable organic carbon, which typically accounts for 70–80% of the

Table 2 Physico-chemical characteristics of soil collected from experimental site

Soil parameters	Typic Haplustalfs (red soil)
pH	6.5
CEC	47.5
Electrical conductivity (dS m^{-1})	0.27
Bulk density (g cm^{-3})	1.41
Organic carbon (g kg^{-1})	4.1
Clay (%)	27
Sand (%)	18
Silt (%)	54
Phosphorus (mg kg^{-1})	4.3
Potassium (mg kg^{-1})	2.3
Calcium (mg kg^{-1})	0.2
Nitrogen (g kg^{-1})	0.8
TOC (g kg^{-1})	0.9
Amorphous Al (g kg^{-1})	1.34
Available Fe (g kg^{-1})	2.1
Available Zn (g kg^{-1})	16.3

actual TOC. Thus, the values reported in this study may be slightly lower than those obtained using high-temperature combustion methods commonly used for TOC determination. Total nitrogen content was determined through Kjeldahl's method.[35] Additionally, nutrient elements such as iron (Fe), aluminium (Al), and zinc (Zn) was extracted by diacid soil digestion and quantified using an atomic absorption spectrophotometer (AAS) as described by Griffith and Schnitzer.[36] The soil's water holding capacity (WHC) was assessed through a percolation test, while soil texture was analyzed using the jar test method. These comprehensive analyses provided a thorough understanding of the soil's properties, essential for the subsequent experimental investigations.

2.3. Sample preparation

The soil samples were prepared by adding Fe-citrate nanoparticles and Zn-citrate nanoparticles, both individually and in combined forms, at concentrations of 250, 500, and 1000 mg kg^{-1}. The nanoparticles and commercial nutrients were thoroughly mixed into the soil to ensure homogeneity, achieved using a mixer for 1-hour post-nutrient addition. Subsequently, the soil samples, both treated and untreated, were moistened to 60% of their water holding capacity (WHC) using sterilized deionized water. These moistened samples were then maintained at a temperature of 22 °C ± 2 °C for an incubation period of 30 days. The impact of aging (contact period) of citrate nanoparticles on soil enzymatic activity was investigated by adding three different concentrations of citrate nanoparticles, followed by incubation and sample collection at various intervals over a 90-day period, reflecting the average duration of agricultural crop growth cycles in India. Samples were collected at three intervals and analyzed for enzymatic activity. Results obtained at all concentrations were compared with those from the 30-day incubation period.

Additionally, a comparative study was conducted to compare the effects of different sources of Fe and Zn, obtained from citrate nanoparticles *versus* commercially available nutrients, at a concentration of 250 mg kg^{-1} of soil. Soil samples were incubated for 30 days while maintaining moisture levels at 60%. After the incubation period, enzymatic activity was assessed and compared. Throughout the experiment, the control sample consisted of untreated soil, free from any chemical additives or nanomaterials. Moisture levels in the soil samples were monitored weekly and adjusted if any deviations were observed. The soil samples used for initial estimation of dehydrogenase and urease activity were stored in darkness at 4 °C. Phosphatase activity was quantified after air-drying the soil samples, following the method outlined by Tabatabai and Bremner.[37]

2.4. Analysis of enzymatic activity

The microbiological quality of soils was estimated through the culture-dependent method and the biochemical quality method (enzymatic activity). Among the two indicators, the enzymatic activity of soils is a highly sensitive indicator and acts as a soil sensor. The enzyme activity of dehydrogenase, urease, acid phosphatase, and alkaline phosphatase was estimated at different intervals of incubation (30, 60, and 90 days), while soil microbiome quantification and diversity analysis were also performed. The enzymatic activity of untreated soil representative sample is given in Table 3.

Briefly, the dehydrogenase activity was determined following the methods outlined in Thalmann's[38] previous reports. Five grams of moist samples were added to a conical glass flask along with calcium carbonate and 1 mL of 3% 2,3,5-triphenyl tetrazolium chloride (TTC) in tris(hydroxymethyl)aminomethane (TRIS) buffer. The flasks were sealed with glass stoppers and incubated shaking in the dark at 37 °C for 24 h. After incubation, 10 mL of methanol was added, and the mixture was shaken for 1 min. The contents were filtered for estimation of absorbance using triphenyl formazan (TPF) as an extracting solution and determined in terms of mg TPF per kg (dry weight soil) per 24 h at a wavelength of 485 nm using a spectrophotometer (BIOTEK). The urease activity was analyzed using the colorimetric technique.[39] Five grams of wet soil were shaken with 0.2 mL toluene in a 50 mL conical flask, sealed with a stopper. Then, 0.05 M of tris(hydroxymethyl)aminomethane (THAM) at pH 9.0 was added, and the contents were kept for 10 min. Later, 2 mL of 0.2 M urea solution was added, mixed well, and incubated at 37 °C for 2 h in the dark. A mixture of 50 mL potassium chloride and silver sulfate solution was added after 2 h of incubation and shaken on a mechanical shaker for another 20 min. Thereafter, urease was measured using the Kjeldahl method for nitrogen content. The urease activity was expressed in terms of mg $N–NH_4^+$ released from 1 kg dry soil for 24 h. Acid and alkaline phosphatase were determined according to the method described by Tabatabai and Bremner (1969)[37] by adding and shaking 0.25 mL of toluene to 1 g of dry soil in a 50 mL Erlenmeyer flask. Four mL of modified universal buffer at pH 6.5 (for acid-phosphatase) or pH 11 (for alkaline phosphatase) and 1 mL of 0.05 M *p*-nitrophenyl phosphate (PNP) aqueous solution were added and incubated for 1 h in the dark at 37 °C. After incubation and addition of 1 mL of 0.5 M $CaCl_2$ and 4 mL 0.5 M NaOH, the solutions were filtered. The filtrate

Table 3 Enzymatic activity of fresh untreated soil sample

Days of incubation	Dehydrogenase [mg TPF per kg d.w. per 24 h]	Urease [mg $N–NH_4^+$ per kg d.w. per 24 h]	Acid phosphatase [mg PNP per kg d.w. per h]	Alkaline phosphatase [mg PNP per kg d.w. per h]
30 days	16.50	37.09	42.22	17.23
60 days	13.33	124.15	43.90	36.95
90 days	11.85	106.26	41.22	21.95

was measured spectrophotometrically at 410 nm wavelength and expressed as mg PNP formed per 1 kg dry soil for 1 h for its phosphatase activity.

2.5. Soil microbiome analysis

2.5.1. Analysis of microbial diversity using culture-dependent techniques. Soil microbiome analysis data is presented in Fig. 11 was conducted using culture-dependent methods, employing specific media for fungi, bacteria, and actinomycetes in all citrate nanoparticles and commercial checks-imposed soil samples. The entire microbiome analysis was carried out at two doses of 250 and 1000 mg kg^{-1} of soil and two incubation periods, *i.e.*, 30 days and 90 days. Microbial count was represented in terms of colony-forming units (CFUs) per gram of soil. The CFUs of the respective dilution were represented in terms of percentage increase or decrease over the untreated sample (control). Ninety milliliters of sterile deionized water were added to ten grams of composite soil sample. The solid and liquid mixture was vortexed for 1 hour for homogenization at 150 rpm. The homogenized solution is termed as the stock solution. The stock solution was used for serial dilution up to seven dilutions for all treated and untreated soil samples. The serial dilutions were plated in three replications and from dilutions of 10^{-2} to 10^{-7} onto respective media for fungi (potato dextrose agar), bacteria (nutrient agar), and actinomycetes (actinomycetes isolation agar). To ensure selective and reproducible isolation, standard protocols were followed for all culture media. For fungal enumeration, potato dextrose agar (PDA; HiMedia) was amended with 50 mg per L streptomycin and 50 mg per L chloramphenicol to suppress bacterial growth. Bacterial populations were assessed using nutrient agar (NA; HiMedia) without selective agents. Actinomycetes were enumerated on Actinomycetes Isolation Agar (AIA; HiMedia), composed of sodium caseinate (2.0 g L^{-1}), L-asparagine (0.1 g L^{-1}), sodium propionate (4.0 g L^{-1}), dipotassium phosphate (0.5 g L^{-1}), magnesium sulfate (0.1 g L^{-1}), ferrous sulfate (0.001 g L^{-1}), glycerol (10.0 g L^{-1}), and agar (15.0 g L^{-1}), pH adjusted to 7.2 ± 0.2. Cycloheximide (50 mg L^{-1}) was added to AIA to inhibit fungal contamination. All media were autoclaved at 121 °C for 20 minutes before use. All media used for microbial count were autoclaved. For plating, the pour plate method was followed. The inoculated plates were incubated for 10 days at 28 °C and counted for colony forming units (CFUs) number. Over-occupied plates were not considered for CFUs count, and only plates with CFUs between 20 and 200 were taken. The colony morphology was studied after 24 hours of incubation at 28 ± 2 °C.

2.6. Data analysis

The average values of three replications were considered and expressed as enzyme activity percentage of treated soil in comparison with the untreated soils. Analysis of variance (ANOVA) was performed at a 5% level of significance among treatments and their replications. All statistical analyses were performed using the SPSS software version. Table 2 presents the enzymatic activity of untreated soils.

3. Results

3.1. Characterization of Fe based NCs using Mössbauer spectroscopy

Mössbauer spectroscopy gives information the chemical nature of and the coordination around the iron species present in the sample. A simple broad doublet indicates that the samples do not possess spontaneous long-range magnetic ordering at room temperature (Fig. 1). This means that no crystalline iron oxide phases are present even as an impurity. The presence of quadrupole doublets suggests that asymmetric coordination sites around Fe. Given the very small particle size distribution,[31] non-equivalent (variously distorted) octahedral environments of Fe nuclei is the cause of large distribution. However, the spectrum is still different from the amorphous Fe_2O_3 spectrum (Table 4). One way to present an definite observation is to measure Mössbauer spectrum at low temperature when the spectrum would still exhibit doublet which may confirm the absence of amorphous Fe_2O_3 phase.[40]

3.2. Effect of nanocitrate (NCs) concentration on soil enzymatic activity

3.2.1. Dehydrogenase activity. Fig. 2 illustrates the relationship between dehydrogenase activity and NCs concentration across all treatments. In T1, enzyme activity showed stimulation from 250 mg kg^{-1} (3.2%) to 500 mg kg^{-1} (6.0%), followed by inhibition at 1000 mg kg^{-1} (2.3%). For T2, the effect varied with concentrations, showing stimulation (8.4%), followed by inhibition (3.2% and 18.9%) at 250, 500, and 1000 mg kg^{-1}, respectively. T3 exhibited inhibition at 250 mg kg^{-1} (8.9%), followed by stimulation at 500 mg kg^{-1} (10.3%) and higher inhibition at 1000 mg kg^{-1} (31.9%). T4, T6, and T7 treatments demonstrated only stimulation. Notably, only T2 and T7 treatments showed a discernible relationship between soil dehydrogenase activity and different NCs concentrations (Fig. 2). In contrast, other treatments (T1, T3, T4, T5, T6) did not

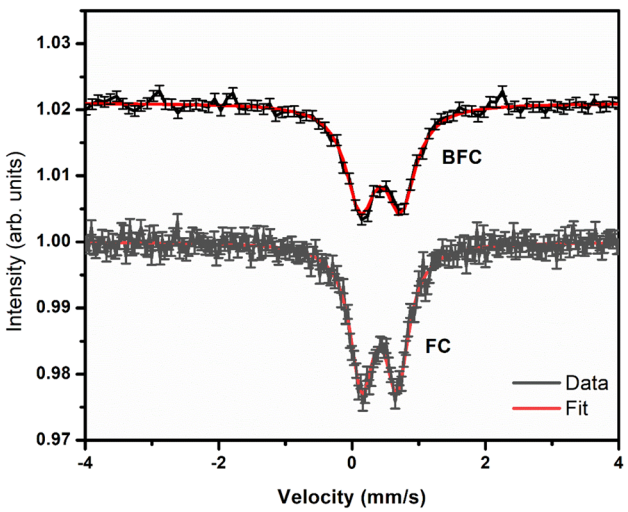

Fig. 1 Room temperature ^{57}Fe Mössbauer spectroscopy data for FC(1 : 1) and BFC(1 : 1)-6 samples.

Table 4 Comparison of Mössbauer spectral fitting parameters obtained in this study and reported literature

Sample	Isomer shift (mm s^{-1})	Quadrupole shift (mm s^{-1})	Width (mm s^{-1})	Ref.
Amorphous Fe_2O_3	0.42(1)	0.93(1)	0.70(1)	50
Ferric citrate	0.40	0.57	—	51
Ferric citrate	0.48(1)	0.63(1)	0.55(3)	52
BFC	0.41(1)	0.53(1)	0.43(2)	This work
FC	0.43(1)	0.60(1)	0.53(2)	This work

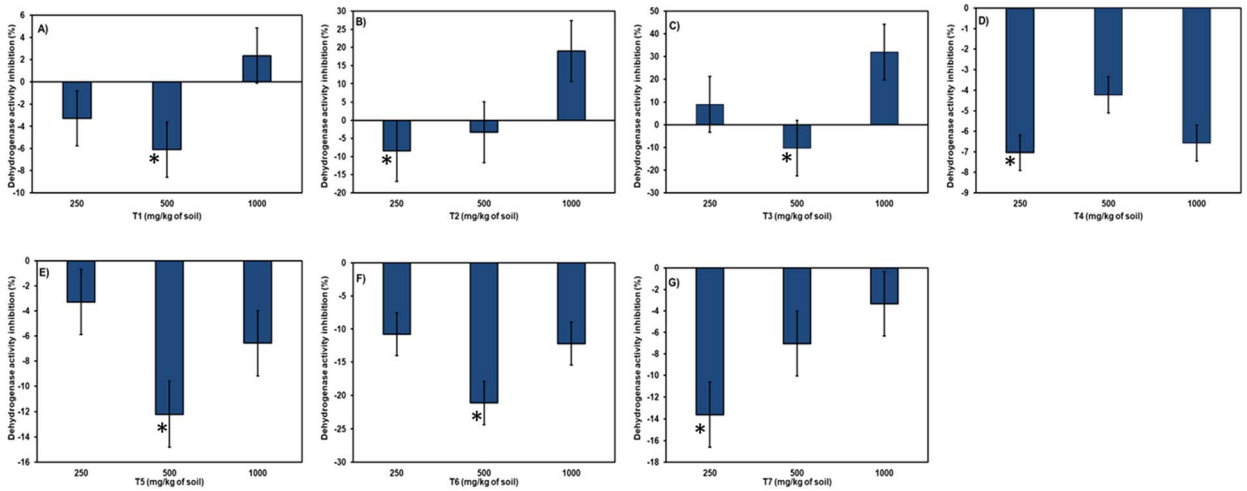

Fig. 2 Dehydrogenase activity in soil (mg TPF per kg dry soil per 24 h) treated with citrate nanoparticles at different concentrations (250, 500, 1000 mg kg^{-1}). Treatments: (A) T1 – BFC(1 : 1)-6, (B) T2 – BZC(1 : 3)-6, (C) T3 – BFZ(4 : 6)-8, (D) T4 – BFZ(5 : 5)-2, (E) T5 – BFZ(5 : 5)-6, (F) T6 – BFZ(8 : 2)-4, (G) T7 – BFCZ(1 : 1 : 1)-6. Error bars represent the standard deviation of the mean ($n = 3$). Enzyme activity was measured as the amount of TPF produced over 24 h in treated soil sample. * – means statistically significant differences ($P \geq 0.05$) between bars.

exhibit any noticeable effect of varying concentrations on dehydrogenase activity. The highest stimulation was depicted from each citrate nanoparticle at lower concentrations like 250 mg kg^{-1} for T2, T4, and T7 treatments, and at 500 mg kg^{-1} for samples like T1, T3, T5, and T6. The stimulation of dehydrogenase activity in the soil with different concentration ranges from 3 to 21%, and it was observed for T6 @ 500 mg kg^{-1} (21.1%). The inhibition of dehydrogenase activity compared to untreated soil ranges from 2.3 to 31.9%, and the highest inhibition was observed in T3 @ 1000 mg kg^{-1} (31.9%). At the highest concentration (1000 mg kg^{-1}) in T1, T2, and T3 treatments of citrate nanoparticles, an inhibition of dehydrogenase enzyme activity was seen, and in remaining citrate nanoparticles of all concentrations resulted in stimulation of dehydrogenase activity. At the highest concentration of NCs (1000 mg kg^{-1}), the highest inhibition or lowest stimulation was

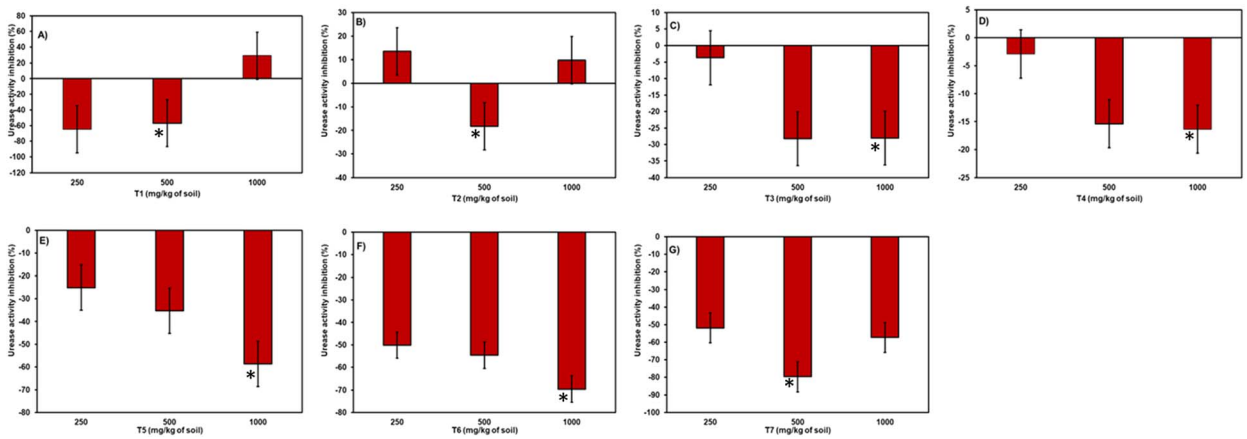

Fig. 3 Effect of studied citrate nanoparticles at different concentrations on urease (A–G) activity in studied soil. Error bars represent the standard deviation of the mean ($n = 3$). * – means statistically significant differences ($P \geq 0.05$) between bars.

observed in all citrate nanoparticles except T4 compared to the other two lower concentrations (250 mg kg^{-1} and 500 mg kg^{-1}).

3.2.2. Urease activity. In experiments with urease, an effect of the NCs concentration was observed (refer to Fig. 3) in all samples except T2 and T7. Among different concentrations, all citrate nanoparticles exhibited a stimulating effect on urease enzyme activity except for T1. The stimulation activity of the urease enzyme ranged from 2.9% to 79.7%. More than 50% enzyme stimulation was observed in certain citrate nanoparticles. The highest stimulation of urease enzyme activity was observed in T7 @ 500 mg kg^{-1} with 79.7%, followed by T6 @ 1000 mg kg^{-1} (69.5%). In T1, a decrease in urease activity with an increase in concentration was observed, with a stimulation effect at 250 mg kg^{-1} (64%) and 500 mg kg^{-1} (56%), and an inhibition effect at 1000 mg kg^{-1} (29%).

In T2 treatment, no effect of concentration was observed, with inhibition at 250 and 1000 mg kg^{-1} (13% and 9%, respectively) and stimulation at 500 mg kg^{-1} (18.3%). In T3, T4, T5, and T6, with an increase in concentration, a strong increase in the stimulation effect of urease enzyme was observed, ranging from 3.1% to 28.2%, 2.9% to 16.3%, 16.3% to 35.2%, and 50.0% to 69.5%, respectively. In T7, there was no effect on urease activity due to its concentration, with the highest stimulation at 500 mg kg^{-1} (79.7%), followed by 1000 mg kg^{-1} (57.3%) and 250 mg kg^{-1} (51.8%), indicating that in all concentrations, more than 50% stimulation of urease enzyme was observed.

3.2.3. Acid phosphatase activity. Contrary to the cases of urease and dehydrogenase, all citrate nanoparticles among the studied concentrations exhibited stimulatory activity of the acid phosphatase enzyme, except for one treatment (T4) at a concentration of 250 mg kg^{-1}, which showed slight inhibition of the enzyme (0.79%) (refer to Fig. 4). In the T1 treatment, the stimulatory effect ranged from 14.7% to 28.1%, with the highest observed at 500 mg kg^{-1}. Similarly, T2 treatment displayed a similar trend in enzyme activity with concentrations, with the highest enzyme activity observed at 500 mg kg^{-1}, ranging from 18.2% to 36.5%. In T3, the effect of concentration on enzyme activity was observed, *i.e.*, with an increase in concentration, the enzyme activity decreased (9.8% to 28.8%). Similar to T3, in T4, the effect of concentration was noticeable, but the stimulating effect increased with an increase in concentration (13.09% to 24.39%), with slight inhibition at 250 mg kg^{-1} (0.79%). The highest enzyme activity (32.6%) was observed in the T5 sample at 1000 mg kg^{-1}. In T6, the highest activity was observed at 250 mg kg^{-1} (28.2%), followed by 1000 mg kg^{-1} (11.8%), and at a soil dose of 500 mg kg^{-1}, the effect was 9.1%. In T7, a slight increase was observed at a soil dose of 500 mg kg^{-1} (26.5%), with equal enzyme activity observed at both concentrations (250 mg kg^{-1} and 1000 mg kg^{-1}).

3.2.4. Alkaline phosphatase activity. In the case of alkaline phosphatase, the NCs (except for T5 @ 250 and 500 mg kg^{-1}; T3 @ 250 mg kg^{-1}; T6 @ 250 and 1000 mg kg^{-1}) displayed an inhibitory effect on alkaline phosphatase enzyme compared to the untreated (refer to Fig. 5). The dose–effect correlation was observed only in the T1, T2, and T3 samples. In T1, T2, and T3, the inhibitory effect increased with the dose increase. The inhibitory effect ranged from 7.7% to 26.2% in T1; 1.5% to 36.7% in T2; and T3 (9.8% to 12.48%), with slight stimulation at the lowest concentration (8.06%). In T4, a more inhibitory effect was observed at all doses compared to other citrate nanoparticles (21.3% to 33.3%). In T5, a stimulation effect was observed at both 250 mg per kg (8.3%) and 500 mg per kg doses (0.59%), with an inhibitory effect at a high dose (15.9%). In T6, a stimulating effect was observed at low (8.3%) and high doses (0.89%), and an inhibitory effect at a 500 mg per kg dose (18.05%). Similar to acid phosphatase, in T7, equal effects were observed at low (1.6%) and high (1.27%) doses, with the highest inhibition at a 500 mg per kg dose (34.05%).

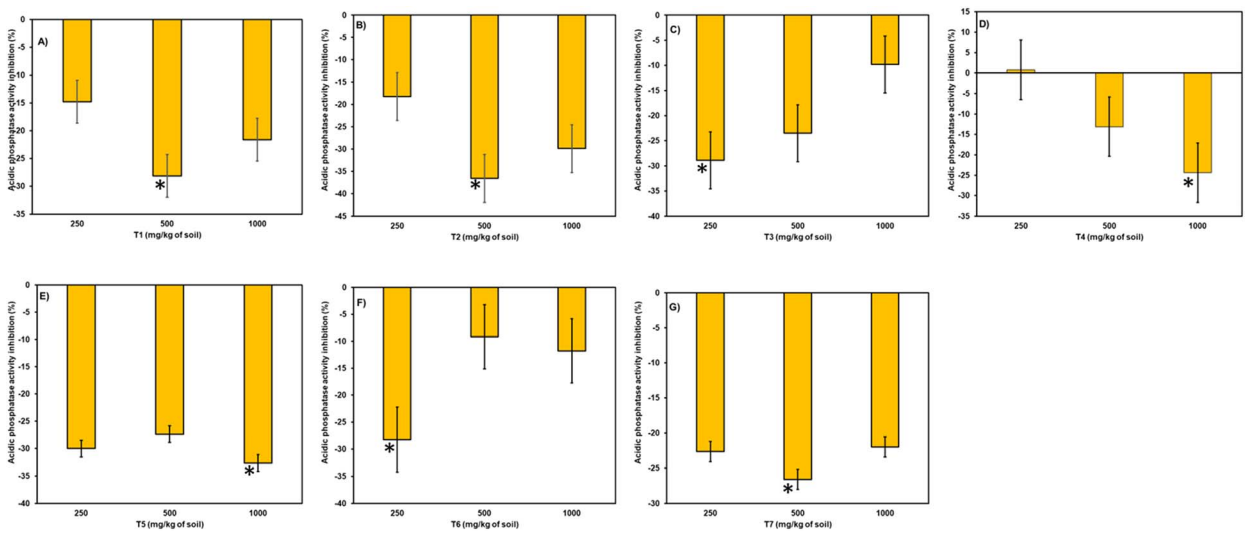

Fig. 4 Effect of studied citrate nanoparticles at different concentrations on acid phosphatase (A–G) activity in studied soil. Error bars represent the standard deviation of the mean ($n = 3$). * – means statistically significant differences ($P \geq 0.05$) between bars.

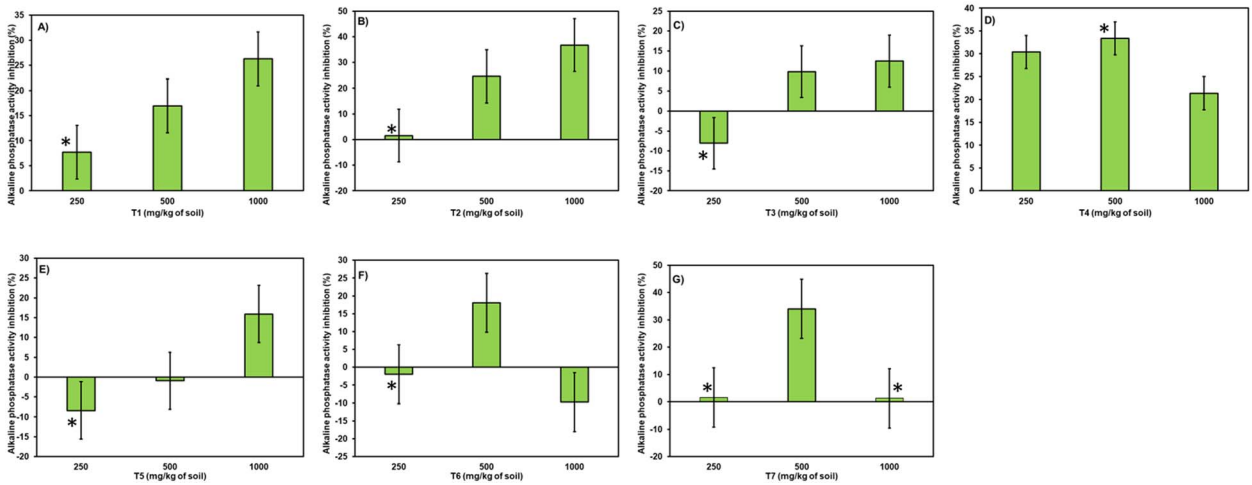

Fig. 5 Effect of studied citrate nanoparticles at different concentrations on alkaline phosphatase (A–G) activity in studied soil. Error bars represent the standard deviation of the mean ($n = 3$). * – means statistically significant differences ($P \geq 0.05$) between bars.

3.3. Influence of NCs–soil contact time on enzymatic activity

A significant effect on all enzyme activities was observed due to the aging of NCs in the soil up to 90 days of incubation (refer to Fig. 6–9). The level of inhibition/stimulation of enzymatic activity differed based on the type and ratio of NCs composition.

Aging/incubation had a stimulating effect across all three concentrations, except for the 60-day period at a higher concentration, where a slight inhibition of 1.16% was observed in the T5 treatment (refer to Fig. 6). At 30 days of incubation, all citrate nanoparticles exhibited stimulation of dehydrogenase enzyme except for T3 at lower (8.9%) and higher doses (31.9%). Over the 60 days of incubation, a varied effect was observed in all samples, with greater inhibition in several citrate nanoparticles across concentrations. However, stimulation was observed in a few samples like T5 at 250 mg kg^{-1} (7.5%) and 500 mg kg^{-1} (13.3%) doses, T6, and T7 in all three concentrations (ranging from 3.4% to 15.11% and 1.7% to 11.04%, respectively). At the end of 90 days of incubation, even toxicity had been converted into stimulation in all citrate nanoparticles, with slighter toxicity retained in T4 at 250 mg per kg dose (2.6%). In some nanocitrate samples at 90 days, inhibition was exhibited after 60 days of stimulation in T6 in all three doses (ranging from 3.2% to 2.6%) and T7 at low (6.5%) and high (11.5%) doses.

The effect of the NCs–soil contact time on urease activity displayed stimulation up to 60 days (refer to Fig. 7). At 30 days and 60 days, stimulation of urease enzyme was observed in all nanocitrate samples, whereas toxicity was observed at 30-day samples like T1 at 1000 mg per kg dose (29.06%) and T2 at lower (13.4%) and higher doses (9.7%). The highest stimulation at 30 days of incubation was observed in T1, T5, T6, and T7 samples compared to 60 days of incubation. At 60 days, the highest stimulation was in T2, T3, and T4 samples. At 90 days of incubation, all stimulation had converted into inhibition of urease

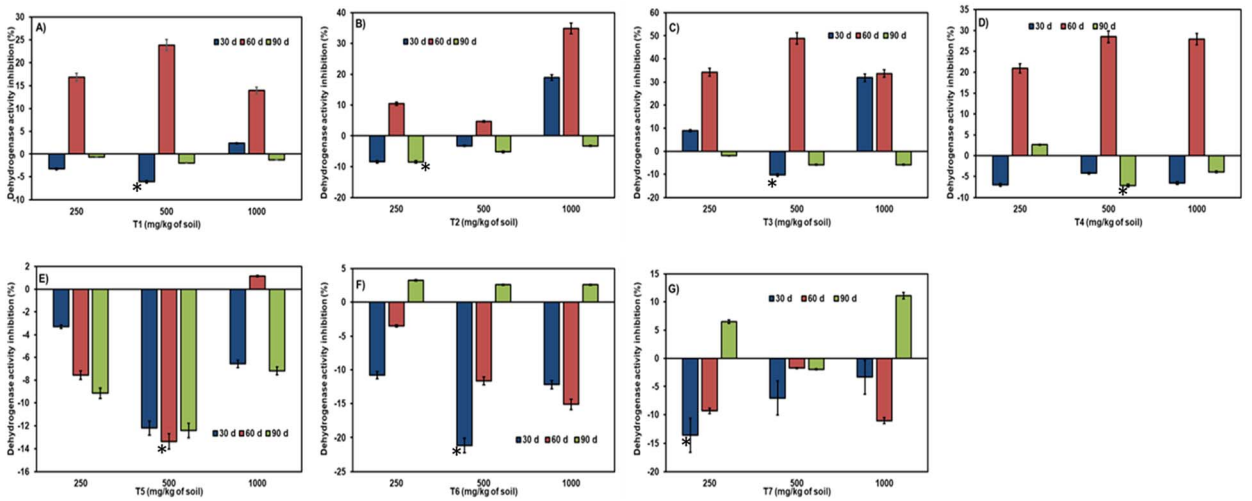

Fig. 6 Effect of NCs aging on dehydrogenase (A–G) activity. Error bars represent the standard deviation of the mean ($n = 3$). * – means statistically significant differences ($P \geq 0.05$) between bars.

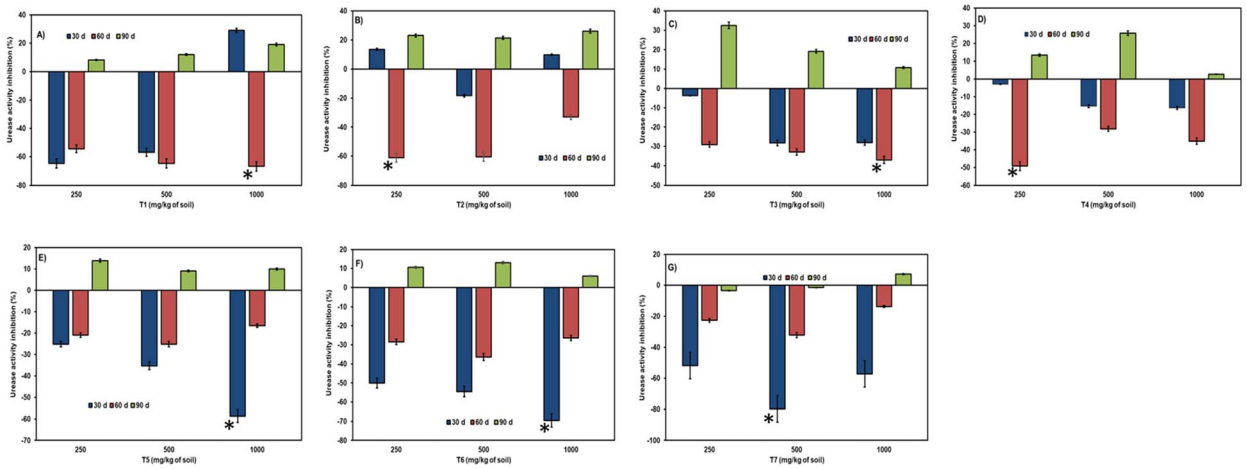

Fig. 7 Effect of NCs aging on urease (A–G) activity. Error bars represent the standard deviation of the mean ($n = 3$). * – means statistically significant differences ($P \geq 0.05$) between bars.

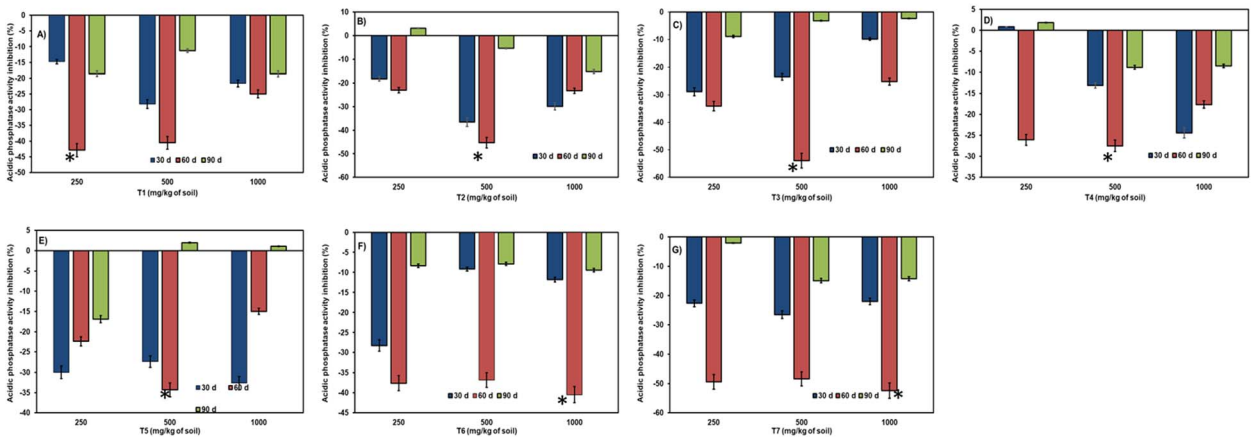

Fig. 8 Effect of NCs aging on acidic phosphatase (A–G) activity. Error bars represent the standard deviation of the mean ($n = 3$). * – means statistically significant differences ($P \geq 0.05$) between bars.

enzyme (except for T7 at 250 mg kg^{-1} (3.5%) and 500 mg kg^{-1} doses (1.5%), where slight stimulation was noticed).

Phosphatase activity resulted in stimulation throughout the entire incubation period and across all three doses (refer to Fig. 8). A notable reduction in stimulation was observed during the 90 days of incubation. The range of enzymatic activity observed was 36.5% to 5.4%, accounting for shorter and longer periods of incubation. At 90 days of incubation, slight inhibition was observed in treatments like T2 at 250 mg kg^{-1}, T4 at 250 mg kg^{-1}, and T5 at 500 and 1000 mg kg^{-1}.

The activity of alkaline phosphatase due to the time of incubation of NCs in soil was not comparable with acid phosphatase (refer to Fig. 9). At 90 days of incubation, statistically significant inhibition was observed compared to considerable stimulation at 60 days of incubation. Only in treatment T1 at a 500 mg per kg dose did the aging period have a positive effect (4.7%) on alkaline phosphatase activity. The range of inhibition observed was between 1.5% to 36.7%, indicating a significant difference.

3.4. Effect of type of source of Fe and Zn nutrient on soil enzymatic activity

The type of Fe and Zn source strongly impacted the enzymatic activity of soils (refer to Fig. 10). Both the NCs and the parameters resulted in a range of differences in enzymatic activity. The sources of Fe and Zn studied included NCs, sulfates of Fe and Zn, EDTA ligand-based Fe and Zn, and nano sources of Fe and Zn. The entire study was conducted at a soil dose of 250 mg kg^{-1}, and the results after 30 days of incubation were compared. Among NCs and other sources, significantly high levels of differences in enzymatic activity were found. While all studied sources exhibited stimulation in acid phosphatase activity, inhibition by commercial sources was observed in other enzymatic activities.

Dehydrogenase enzymatic activity varied considerably due to the effect of the NCs and commercial checks in soil (refer to Fig. 10A). Greater stimulation of dehydrogenase activity was observed with NCs, irrespective of their ratio of Fe and Zn, compared to commercial nutrients of Fe and Zn. Among the

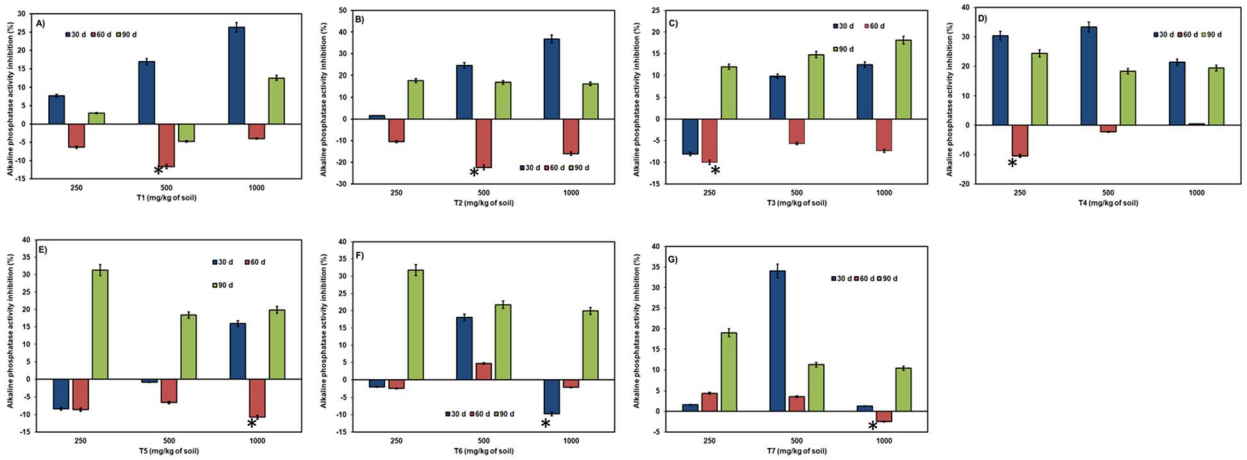

Fig. 9 Effect of NCs aging on alkaline phosphatase (A–G) activity. Error bars represent the standard deviation of the mean ($n = 3$). * – means statistically significant differences ($P \geq 0.05$) between bars.

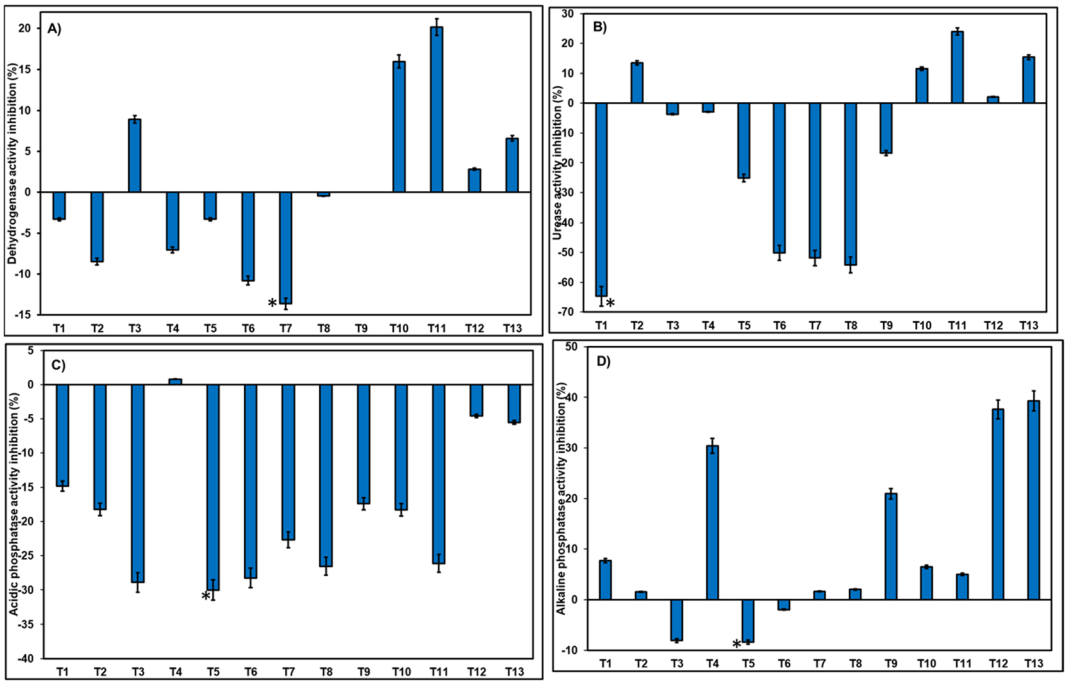

Fig. 10 The effect of source of Fe and Zn on enzyme (A) dehydrogenase (B) urease (C) acid phosphatase and (D) alkaline phosphatase of investigated soils. Error bars represent the standard deviation of the mean ($n = 3$). * – means statistically significant differences ($P \geq 0.05$) between bars.

NCs, stimulation was greater than that of commercial nutrients, except in treatment T3, which exhibited 8.9% inhibition. The range of inhibition varied from no activity to 20.18% in soils containing commercial nutrients, whereas the range of stimulation ranged from 3.2% to 33.7% in soils treated with citrate nanoparticles.

More variability of urease enzymatic activity was observed than dehydrogenase in soils due to the type of Fe and Zn nutrient source. NCs caused greater stimulation or lower inhibition of urease activity in soils compared to commercial checks (refer to Fig. 10B). T3 and T4 treatments of NCs showed no significant urease activity. The range of toxicity or inhibition was minimal, ranging from 11.5% to 13.4%, irrespective of the type of Fe and Zn source. Even the checks like ferrous sulfate (54.1%) and zinc sulfate (16.7%) exhibited stimulation of urease compared to other checks.

No significant disparities were observed in acid phosphatase activity in soils treated with NCs compared to those treated with commercial nutrients (refer to Fig. 10C). Both NCs and commercial nutrients led to the stimulation of enzyme activity, unlike other enzymatic activities. Notably, Fe-EDTA and Zn-EDTA showed less stimulation compared to the other studied

nutrients. Additionally, in T4 treatment, a slight inhibition of acid phosphatase activity was observed compared to other samples (0.79%).

The alkaline phosphatase activity was largely influenced by the type of Fe and Zn nutrient source and the form of the compound (refer to Fig. 10D). In the studied soil sample, Fe and Zn resulted in an inhibition of alkaline phosphatase activity. Few citrate samples like T3 (8.06%), T5 (8.37%), and T6 treatments exhibited slight stimulation, *i.e.*, below 10%. The highest inhibition was exhibited by chelated Fe and Zn, with 37.6% and 39.2%, respectively. However, toxicity was noted to a higher extent (by 30.3%) in the case of the T4 nanocitrate treatment.

3.5. Soil microbiome analysis

Soil microbiome analysis data is presented in Fig. 11. Actinomycetes were the most affected microbial group, followed by fungi, in all treated samples, while bacteria remained unaffected or less affected. At 30 days, fungal abundance was highest in BFC(1 : 1)-6 with a 85.71% increase, while 100% abundance was observed in T4 for actinomycetes, and bacterial abundance was 100% in all samples. Compared to the 30-day incubation period, a decrease in the count was observed in actinomycetes and bacteria at the end of the 90-day incubation, with a slight increase in fungal abundance. At higher doses and after 90 days

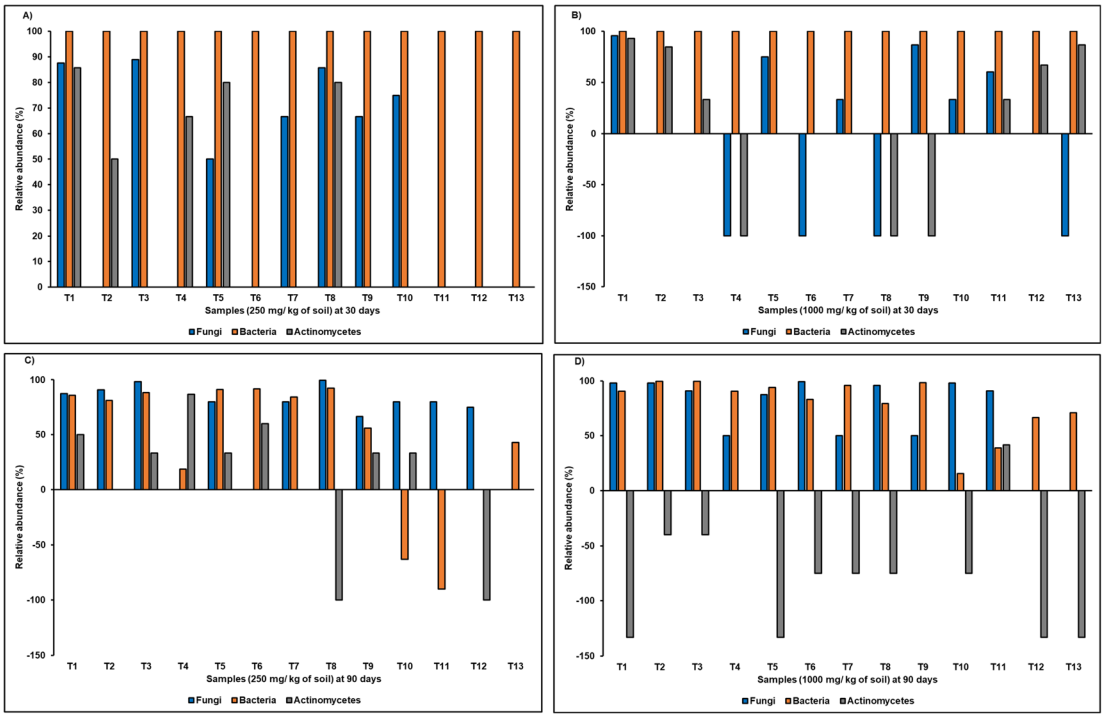

Fig. 11 Microbial taxonomic composition of cultivable fractions of soil microbiome after imposition of treatments at (A) 250 mg kg^{-1} of soil at 30 days; (B) 1000 mg kg^{-1} of soil at 30 days; (C) 250 mg kg^{-1} of soil at 90 days; and (D) 1000 mg kg^{-1} of soil at 30 days.

Table 5 Diversity composition of cultivable fractions of soil microbiome after imposition of treatments at 30 days of incubation

	250 mg			1000 mg		
Nutrient	Fungi	Bacteria	Actinomycetes	Fungi	Bacteria	Actinomycetes
BFC(1 : 1)-6	12	10	2	8	6	2
BZC(1 : 3)-6	5	12	2	4	5	1
BFZ(4 : 6)-8	3	11	1	2	7	1
BFZ(5 : 5)-2	4	10	2	6	5	1
BFZ(5 : 5)-6	3	10	2	1	4	0
BFZ(8 : 2)-4	5	12	3	6	5	1
BFCZ(1 : 1 : 1)-6	4	8	0	7	6	1
$FeSO_4$	4	10	2	3	7	1
$ZnSO_4$	7	11	1	5	5	1
Nano Fe	3	5	0	6	5	1
Nano Zn	2	6	0	6	6	3
Chelated-Fe	4	6	0	5	3	2
Chelated-Zn	3	5	0	6	4	1
Untreated	5	4	1	6	3	1

Table 6 Diversity composition of cultivable fractions of soil microbiome after imposition of treatments at 90 days of incubation

Nutrient	250 mg			1000 mg		
In CFUs	Fungi	Bacteria	Actinomycetes	Fungi	Bacteria	Actinomycetes
BFC(1 : 1)-6	5	10	1	7	5	1
BZC(1 : 3)-6	8	9	1	8	6	1
BFZ(4 : 6)-8	6	10	1	6	4	2
BFZ(5 : 5)-2	8	7	1	6	6	1
BFZ(5 : 5)-6	9	9	1	3	5	1
BFZ(8 : 2)-4	4	10	2	7	3	1
BFCZ(1 : 1 : 1)-6	6	11	0	2	7	1
$FeSO_4$	2	7	1	7	4	1
$ZnSO_4$	2	5	1	6	5	1
Nano Fe	4	8	1	4	6	1
Nano Zn	7	7	1	4	10	1
Chelated-Fe	3	6	1	5	11	1
Chelated-Zn	5	5	1	4	7	1
Untreated	2	6	0	2	8	1

of incubation, inhibition of actinomycetes count was observed. Microbial diversity analysis was represented in Tables 5 and 6.

3.6. Correlation between enzyme activities and microbial abundance

To explore the relationship between soil biological functions and microbial communities, Pearson correlation analysis was conducted between enzyme activities (dehydrogenase, urease, acid and alkaline phosphatases) and CFU counts of bacteria, fungi, and actinomycetes across treatments (Fig. 12).

The analysis revealed a significant positive correlation between bacterial CFU and urease activity ($r = 0.82$, $p < 0.01$), suggesting a close link between microbial biomass and nitrogen cycling processes. Dehydrogenase activity was moderately correlated with both bacterial ($r = 0.68$) and fungal abundance ($r = 0.71$), reflecting its intracellular nature and sensitivity to microbial respiration. Acid phosphatase showed a weak but positive correlation with actinomycetes ($r = 0.55$), while alkaline phosphatase activity did not show strong correlations with any single microbial group.

These correlations suggest that the functional shifts in enzyme activity are at least partly driven by changes in microbial abundance and composition due to nanoparticle treatments. The findings strengthen the mechanistic link between nanoparticle-induced microbial responses and observed biochemical changes in soil.

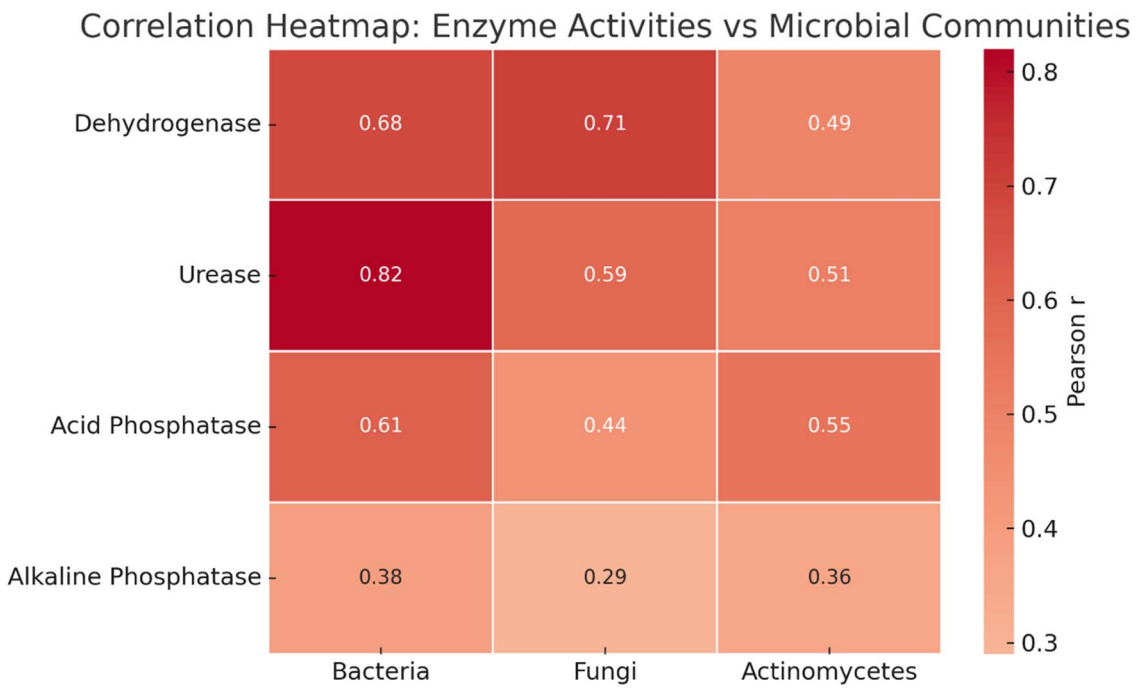

Fig. 12 Correlation heatmap of enzyme activities and microbial communities. All values represent Pearson correlation coefficients (*r*). Highest values indicate significant correlation at $p < 0.01$.

4. Discussion

Based on the concentration of NCs, the effect on the soil enzymatic activity was strongly diversified. Along with the concentration of NCs, the enzymatic activity was influenced due to soil properties, the type of enzyme studied, and the composition of citrate nanoparticles. Based on the results, the citrate nanoparticles were strongly negatively influenced by specific enzymes. The combined citrates do not have an inhibitory effect on the dehydrogenase enzyme (except T3). This could be due to a slightly higher content of zinc available than of Fe. In earlier reports, the sensitivity of zinc oxide nanoparticles has been observed on various enzymes.[4,41] The combined citrates in studied enzymes do not have much inhibition, whereas individual citrates (T1 and T2) have shown sensitivity at higher concentrations. As it is a laboratory experiment with controlled conditions and without any plant–soil interaction, the inhibition of enzymes might be possible at higher concentrations. Under field studies, with a single dose of nutrients, additional interaction of plant and external environmental influence can stimulate enzymatic activity at higher concentrations.[42] Furthermore, in specific treatments such as T2, a non-monotonic or biphasic pattern was observed in urease and alkaline phosphatase activities, where both 250 and 1000 mg per kg doses showed stimulation while the intermediate dose of 500 mg kg^{-1} did not. This behavior may result from nanoparticle aggregation dynamics, concentration-dependent ligand–metal interactions, microbial stress responses, or modulation by soil physico-chemical properties. Over time, the slight negative effect may be reduced due to the continuous buildup of NCs by plants and also reduce the range of exposure.[4,43] In field studies under cucumber, the influence of nanoparticles on soil enzymatic activity has been studied and showed a reduction in effect on enzymatic activity in a particular soil type.[41] These results will encourage the study of the effect of nanomaterials under soil types with diversified properties, which truly gives the toxicity or stimulating effect. The scale of effect on enzymatic activity may change due to the aging period of NCs in the soils.[6,44,45] Due to ligand-based nanosystems, the citrate nanoparticles do not realize sorption or reaction with clay or other natural organic particles in the soil, which amplifies the probability of mobilization. A reduction of enzymatic activity was observed with the increased NCs–soil contact period in the present study. It indirectly indicates the availability of NCs in soils and ensures their exposure by plants when grown around.[19,44] The lower bioavailability of NCs and ions, which are key components of the enzymes, can be confirmed due to the reduction in stimulating effect over time.[46] Soil enzymatic activity is significantly influenced by the source of Fe and Zn, as well as the type of enzyme being studied. The dehydrogenase enzyme, being more sensitive and intracellular, serves as a crucial indicator of soil contamination, responding differently to various contaminants compared to extracellular enzymes.[14,47,48] Extracellular enzymes like urease and phosphatases (both acidic and alkaline) are primarily affected by the physico-chemical properties of soils, unlike dehydrogenase enzymes.[14,17] The adsorption of extracellular enzymes by natural organic matter and clays obstructs nutrient and ion contact with the enzymes. Soil properties such as pH, organic matter content, clay composition, and mineral content, along with their antagonistic and synergistic effects, play pivotal roles in determining the impact of nutrients on soil enzymatic activity.[9,14–16,19,23] The electrostatic forces and hydrophobic interactions of soil organic acids with nutrients also influence soil enzymes,[49] potentially reducing nutrient bioavailability to plants and soil enzyme activity. Nutrient ions released may lead to immobilization due to reactions with organic matter functional groups.[19] The significant stimulation observed with citrates suggests their mobilization in soil rather than sorption onto organic matter. Market-available sources of Fe and Zn exhibit reactivity with organic matter, leading to enzyme activity inhibition and toxicity. Generally, the composition and diversity of the cultivatable fractions of the microbial communities were affected by many factors. Isolation medium, cultivation protocol, media agents, treatment effect, and soil type are some important factors for soil microbiome analysis. While this study provides valuable insights into the impact of citrate-based nanoparticles on soil microbiota using culture-dependent methods, we acknowledge the inherent limitations of this approach. Culture-dependent techniques, although useful for quantifying cultivable microbial groups such as fungi, bacteria, and actinomycetes, fail to capture the vast majority of unculturable microorganisms and often underrepresent microbial diversity and functional potential. As a result, key shifts in microbial community structure, rare taxa, and functional gene expressions may remain undetected. Furthermore, colony morphology alone cannot provide species-level resolution or insight into ecological functions or metabolic capacities.

To overcome these limitations and enable a more comprehensive understanding of microbial responses to chelated nanoparticles, future studies should integrate culture-independent, high-throughput sequencing approaches such as 16S rRNA gene amplicon sequencing, ITS sequencing for fungi, and metagenomics. These methods would allow for deeper taxonomic profiling, identification of non-culturable organisms, and insight into functional pathways influenced by nanoparticle exposure. Additionally, incorporating qPCR assays targeting nutrient cycling genes or stress markers could further elucidate the functional impact of nanocitrates on the soil microbiome. Such approaches would greatly enhance the ecological relevance and mechanistic understanding of nanoparticle–microbiome interactions in agroecosystems. While this study provides valuable insights into the impact of citrate-based nanoparticles on soil microbiota using culture-dependent methods, we acknowledge the inherent limitations of this approach. Culture-dependent techniques, although useful for quantifying cultivable microbial groups such as fungi, bacteria, and actinomycetes, fail to capture the vast majority of unculturable microorganisms and often underrepresent microbial diversity and functional potential. As a result, key shifts in microbial community structure, rare taxa, and functional gene expressions may remain undetected. Furthermore, colony

morphology alone cannot provide species-level resolution or insight into ecological functions or metabolic capacities.

To overcome these limitations and enable a more comprehensive understanding of microbial responses to chelated nanoparticles, future studies should integrate culture-independent, high-throughput sequencing approaches such as 16S rRNA gene amplicon sequencing, ITS sequencing for fungi, and metagenomics. These methods would allow for deeper taxonomic profiling, identification of non-culturable organisms, and insight into functional pathways influenced by nanoparticle exposure. Additionally, incorporating qPCR assays targeting nutrient cycling genes or stress markers could further elucidate the functional impact of nanocitrates on the soil microbiome. Such approaches would greatly enhance the ecological relevance and mechanistic understanding of nanoparticle–microbiome interactions in agroecosystems. In a few treatments of citrate nanoparticles, a positive increase over control can be a good sign, and the little effect on exposure to real field studies will be lessened.

These findings of the correlation support the conclusion that nanocitrate-induced shifts in soil enzymatic functions are closely linked to microbial abundance and community structure. The positive correlations strengthen the hypothesis that citrate nanoparticles, especially at optimized concentrations, enhance microbial-mediated nutrient cycling rather than disrupting microbial communities. This integrated biochemical and microbiological perspective adds mechanistic depth to the observed biosafety of nanocitrates and supports their application as sustainable nutrient inputs in soil ecosystems.

The behavior and efficacy of citrate-based Fe and Zn nanoparticles are strongly influenced by the physico-chemical properties of the soil matrix. The present study was conducted using Indian red soil with a mildly acidic pH of 6.5 (Table 2), which plays a critical role in nanoparticle solubility, nutrient availability, and microbial interactions. In acidic soils, iron and zinc exhibit higher solubility, and citrate ligands enhance this further by complexing metal ions, preventing precipitation as hydroxides or phosphates. This contributes to the observed enhanced enzyme activities and microbial proliferation, particularly for urease and dehydrogenase.

However, the behavior of nanocitrates may differ significantly in alkaline or calcareous soils, where metal ion solubility is reduced due to increased formation of insoluble hydroxides and carbonates. In such soils, citrate chelation may help mitigate metal immobilization, but adsorption to negatively charged clay particles and organic matter may limit bioavailability. Additionally, pH-mediated shifts in microbial community composition and enzyme expression could alter biological responses. Thus, while the current results demonstrate biosafety and efficacy under acidic conditions, further validation across diverse soil types is warranted to assess nanoparticle stability, mobility, and functional performance under variable pH and mineralogical conditions.

5. Conclusion

This study evaluated the biosafety of chelated Fe and Zn citrate nanoparticles applied to Indian red soil (pH 6.5), with a focus on their impact on soil enzyme activity and microbial diversity. Unlike conventional metal oxide nanoparticles, these citrate-based nanonutrients are amorphous, ligand-based formulations with particle sizes below 120 nm and negative zeta potential (−28 to −35 mV), providing improved solubility and reduced aggregation under soil conditions. Across treatments, citrate nanoparticles at concentrations ≤500 mg kg^{-1} resulted in >90% of enzyme activity changes remaining within ±20% of the control values, indicating minimal disturbance to microbial functioning. Strong positive correlations were observed between urease activity and bacterial CFU ($r = 0.82$), and between dehydrogenase and fungal/bacterial counts, supporting a link between microbial abundance and functional enzymatic responses. The study soil—acidic Indian red soil (pH 6.5)—favored metal solubility and microbial activity, enabling effective release and utilization of nutrients from the nanocitrates. However, the performance and interaction of these nanomaterials may vary in alkaline or calcareous soils, where reduced solubility and increased adsorption may limit efficacy. These findings highlight the need for site-specific evaluation of nanoparticle formulations under diverse soil pH and mineralogical contexts. In conclusion, citrate-chelated Fe and Zn nanoparticles represent a promising biosafe alternative for micronutrient delivery *via* soil application. Their low toxicity, soil compatibility, and targeted microbial interactions position them as environmentally sustainable inputs in precision agriculture, though further validation under diverse agroecosystems is warranted.

While the findings provide strong evidence of biosafety and functional compatibility of citrate nanoparticles in acidic soil under controlled conditions, this study is limited by its use of a single soil type (Indian red soil, pH 6.5) and a short-term incubation period (90 days). These constraints do not account for long-term cumulative effects, potential interactions with other soil components (*e.g.*, organic matter, clay minerals), or the influence of crop rhizosphere activity. Therefore, field-scale, multi-season trials across diverse agro-climatic zones and soil types are needed to evaluate the persistence, transformation, and agroecological impacts of nanocitrates under realistic agricultural conditions.

Data availability

The data supporting this article have been included as part of the ESI.†

Author contributions

KSVP conceptualized the work, wrote the original draft, reviewed and edited the manuscript draft. BG supervised, reviewed and edited the manuscript. RDP and AS reviewed the manuscript draft.

Conflicts of interest

The authors declare no competing financial interests.

Acknowledgements

We acknowledge DST, Govt of India, for DST FIST grant number FST/CSI-240/2012 and the central analytical facility at BITS Pilani Hyderabad campus. We acknowledge ICAR-IIOR for extending the facilities to conduct enzymatic studies. We immensely thank Dr V. Raghavendra Reddy, UGC-DAE Consortium for Scientific Research, Indore, India for the Mössbauer measurements and data fitting.

References

1 S. J. Klaine, P. J. J. Alvarez, G. E. Batley, T. F. Fernandes, R. D. Handy, D. Y. Lyon, S. Mahendra, M. J. McLaughlin and J. R. Lead, Nanomaterials in the environment: behavior, fate, bioavailability, and effects, *Environ. Toxicol. Chem.*, 2008, **27**, 1825–1851.

2 F. Gottschalk and B. Nowack, The release of engineered nanomaterials to the environment, *J. Environ. Monit.*, 2011, **13**, 1145–1155.

3 D. M. Auffan, D. C. Santaella, P. A. Thiéry, C. Paillès, J. Rose, D. W. Achouak, D. A. Thill, A. Masion, M. Wiesner and J. Y. Bottero, Ecotoxicity of inorganic nanoparticles: from unicellular organisms to invertebrates, in *Encyclopedia of Nanotechnology*, ed. Bhushan, P. B., Springer, Netherlands, 2012, pp. 623–636.

4 W. Du, Y. Sun, R. Ji, J. Zhu, J. Wu and H. Guo, TiO_2 and ZnO nanoparticles negatively affect wheat growth and soil enzyme activities in agricultural soil, *J. Environ. Monit.*, 2011, **13**, 822–828.

5 Y. Ge, J. P. Schimel and P. A. Holden, Identification of soil bacteria susceptible to TiO2 and ZnO nanoparticles, *Appl. Environ. Microbiol.*, 2012, **78**, 6749–6758.

6 I. Jośko and P. Oleszczuk, Influence of soil type and environmental conditions on ZnO, TiO_2 and Ni nanoparticles phytotoxicity, *Chemosphere*, 2013, **92**, 91–99.

7 O. Choi, K. K. Deng, N. J. Kim, J. L. Ross, R. Y. Surampalli and Z. Hu, The inhibitory effects of silver nanoparticles, silver ions, and silver chloride colloids on microbial growth, *Water Res.*, 2008, **42**, 3066–3074.

8 Y. Ge, J. P. Schimel and P. A. Holden, Evidence for negative effects of TiO_2 and ZnO nanoparticles on soil bacterial communities, *Environ. Sci. Technol.*, 2011, **45**, 1659–1664.

9 L. Vittori Antisari, S. Carbone, A. Gatti, G. Vianello and P. Nannipieri, Toxicity of metal oxide (CeO_2, Fe_3O_4, SnO_2) engineered nanoparticles on soil microbial biomass and their distribution in soil, *Soil Biol. Biochem.*, 2013, **60**, 87–94.

10 Y. Tingting, L. Dandan, C. Jing, Y. Zhongzhou, D. Runzhi, G. Xiang and W. Li, Effects of metal oxide nanoparticles on soil enzyme activities and bacterial communities in two different soil types, *J. Soils Sediments*, 2018, **18**, 211–221.

11 B. M. Tal, F. Sammy, D. Ishai, M. Dror and B. Brian, Effects of metal oxide nanoparticles on soil properties, *Chemosphere*, 2013, **90**, 640–646.

12 K. V. Sandeep, K. D. Ashok, K. P. Manoj, S. Ashish, K. Vinay and G. Saikat, Engineered nanomaterials for plant growth and development: A perspective analysis, *Sci. Total Environ.*, 2018, **630**, 1413–1435.

13 H. Ghafari and J. Razmjoo, Effect of Foliar Application of Nano-iron Oxidase, Iron Chelate and Iron Sulphate Rates on Yield and Quality of Wheat, *Int. J. Agron. Plant Prod.*, 2013, **4**(11), 2997–3003.

14 M. A. Aon and A. C. Colaneri, Temporal and spatial evolution of enzymatic activities and physico-chemical properties in an agricultural soil, *Appl. Soil Ecol.*, 2001, **18**, 255–270.

15 R. G. Burns, J. L. DeForest, J. Marxsen, R. L. Sinsabaugh, M. E. Stromberger, M. D. Wallenstein, M. N. Weintraub and A. Zoppini, Soil enzymes in a changing environment: current knowledge and future directions, *Soil Biol. Biochem.*, 2013, **58**, 216–234.

16 R. Dinesh, M. Anandaraj, V. Srinivasan and S. Hamza, Engineered nanoparticles in the soil and their potential implications to microbial activity, *Geoderma*, 2012, 19–27.

17 P. M. Huang, M. K. Wang and C. Y. Chiu, Soil mineral–organic matter–microbe interactions: impacts on biogeochemical processes and biodiversity in soils, *Pedobiologia*, 2005, **49**, 609–635.

18 L. Jin, Y. Son, T. K. Yoon, Y. J. Kang, W. Kim and H. Chung, High concentrations of single-walled carbon nanotubes lower soil enzyme activity and microbial biomass, *Ecotoxicol. Environ. Saf.*, 2013, **88**, 9–15.

19 C. Peyrot, K. J. Wilkinson, M. Desrosiers and S. Sauvé, Effects of silver nanoparticles on soil enzyme activities with and without added organic matter, *Environ. Toxicol. Chem.*, 2014, **33**, 115–125.

20 B. Shrestha, V. Acosta-Martinez, S. B. Cox, M. J. Green, S. Li and J. E. Cañas-Carrell, An evaluation of the impact of multiwalled carbon nanotubes on soil microbial community structure and functioning, *J. Hazard. Mater.*, 2013, **261**, 188–197.

21 S. Kim, H. Sin, S. Lee and I. Lee, Influence of metal oxide particles on soil enzyme activity and bioaccumulation of two plants, *J. Microbiol. Biotechnol.*, 2013, **23**, 1279–1286.

22 P. Oleszczuk and H. Hollert, Comparison of sewage sludge toxicity to plants and invertebrates in three different soils, *Chemosphere*, 2011, **83**, 502–509.

23 B. Pan and B. Xing, Applications and implications of manufactured nanoparticles in soils: a review, *Eur. J. Soil Sci.*, 2012, **63**, 437–456.

24 M. Horie, K. Nishio, S. Endoh, H. Kato, K. Fujita, A. Miyauchi, A. Nakamura, S. Kinugasa, K. Yamamoto, E. Niki, Y. Yoshida and H. Iwahashi, Chromium(III) oxide nanoparticles induced remarkable oxidative stress and apoptosis on culture cells, *Environ. Toxicol.*, 2013, **28**, 61–75.

25 B. Nowack and T. D. Bucheli, Occurrence, behavior and effects of nanoparticles in the environment, *Environ. Pollut.*, 2007, **150**, 5–22.

26 M. A. Dar and S. S. Andrabi, Nanoparticles in the production of algae, in *Nanotech Bioenergy Biofuel Prodn*, ed. M. Maqbool Rather, P. Ahmad, M. Iqbal Lone and A. L. Lone, CRC Press, 2023.

27 S. Kaliamurthi, G. Selvaraj and B. Bhaskar, Viewing the emphasis on state-of-the-art magnetic nanoparticles:

Synthesis, physical properties, and applications in cancer theranostics, *J. Drug Delivery Sci. Technol.*, 2019, **49**, 681–689.
28 V. D. Rajput, T. Minkina and S. Sushkova, Effect of nanoparticles on crops and soil microbial communities, *J. Soils Sediments*, 2018, **18**, 2179–2187.
29 U. S. Ezealigo, B. N. Ezealigo, S. O. Aisida and F. I. Ezema, Iron oxide nanoparticles in biological systems: antibacterial and toxicology perspective, *JCIS Open*, 2021, **4**, 100027.
30 M. Becana, J. F. Moran and I. Iturbe-Ormaetxe, Iron-dependent oxygen free radical generation in plants subjected to environmental stress: toxicity and antioxidant protection, *Plant Soil*, 1998, 137–147.
31 K. S. V. P. Chandrika, D. Patra, P. Yadav, A. A. Qureshi and B. Gopalan, Metal citrate nanoparticles: a robust water-soluble plant micronutrient source, *RSC Adv.*, 2021, **11**, 20370, DOI: **10.1039/D1RA02907J**.
32 K. S. V. P. Chandrika, A. A. Qureshi, A. Singh, S. Chunduri and B. Gopalan, Fe and Zn metal nanocitrates as plant nutrients through soil application, *ACS Omega*, 2022, 7(49), 45481–45492, DOI: **10.1021/acsomega.2c06096**.
33 K. S. V. P. Chandrika, A. A. Qureshi and B. Gopalan, Fe and Zn citrate nanoparticles: leaching and vertical distribution in column of Indian red soils, *Heliyon*, 2024, **10**(19), e38546.
34 L. P. van Reeuwijk, *Procedures for Soil Analysis*, International Soil Reference and Information Centre, 1993.
35 J. M. Bremner, *Nitrogen — Total*, 1996, pp. 1085–1121.
36 S. M. Griffith and M. Schnitzer, Analytical characteristics of humic and fulvic acids extracted from tropical volcanic soils, *Soil Sci. Soc. Am. J.*, 1975, **39**, 861.
37 M. A. Tabatabai and J. M. Bremner, Use of p-nitrophenyl phosphate for assay of soil phosphatase activity, *Soil Biol. Biochem.*, 1969, **1**, 301–307.
38 A. Thalmann, Zur methodik der Bestimmung der dehydrogenase activität in Boden mittels triphenyltetrazoliumchlorid (TTC), *Landwirtsch. Forsch.*, 1968, 249–258.
39 M. I. Zantua and J. M. Bremner, Comparison of methods of assaying urease activity in soils, *Soil Biol. Biochem.*, 1975, **7**, 291–295.
40 L. Machala, J. Tuček and R. Zbořil, Polymorphous transformations of nanometric iron(III) oxide: A review, *Chem. Mater.*, 2007, **19**(18), 4562–4577, DOI: **10.1021/cm070405f**.
41 S. Kim, J. Kim and I. Lee, Effects of Zn and ZnO nanoparticles and Zn^{2+} on soil enzyme activity and bioaccumulation of Zn in Cucumis sativus, *Chem. Ecol.*, 2011, **27**, 49–55.
42 I. Jośko, P. Oleszczuk and B. Futa, The effect of inorganic nanoparticles (ZnO, Cr_2O_3, CuO and Ni) and their bulk counterparts on enzyme activities in different soils, *Geoderma*, 2014, 232–234.
43 J. H. Priester, Y. Ge, R. E. Mielke, A. M. Horst, S. C. Moritz, K. Espinosa, J. Gelb, S. L. Walker, R. M. Nisbet, Y. J. An, J. P. Schimel, R. G. Palmer, J. A. Hernandez-Viezcas, L. Zhao, J. L. GardeaTorresdey and P. A. Holden, Soybean susceptibility to manufactured nanomaterials with evidence for food quality and soil fertility interruption, *Proc. Natl. Acad. Sci. U. S. A.*, 2012, **109**, E2451–E2456.
44 C. Coutris, E. J. Joner and D. H. Oughton, Aging and soil organic matter content affect the fate of silver nanoparticles in soil, *Sci. Total Environ.*, 2012, **420**, 327–333.
45 I. A. Mudunkotuwa, J. M. Pettibone and V. H. Grassian, Environmental implications of nanoparticle aging in the processing and fate of copper-based nanomaterials, *Environ. Sci. Technol.*, 2012, **46**, 7001–7010.
46 J. C. Polacco, P. Mazzafera and T. Tezotto, Opinion — nickel and urease in plants: still many knowledge gaps, *Plant Sci.*, 2013, **199**, 79–90.
47 R. P. Dick, Soil enzyme activities as integrative indicators of soil health, In *Biological Indicators of Soil Health*, ed. C. E. Pankhurst, B. M. Doube, V. V. S. R. Gupta, CAB International, Wallingford, 1997, pp. 121–156.
48 J. E. Rogers and S. W. Li, Effect of metals and other inorganic ions on soil microbial activity: soil dehydrogenase assay as a simple toxicity test, *Bull. Environ. Contam. Toxicol.*, 1985, **34**, 858–865.
49 E. Navarro, A. Baun, R. Behra, N. B. Hartmann, J. Filser, A. J. Miao, A. Quigg, P. H. Santschi and L. Sigg, Environmental behavior and ecotoxicity of engineered nanoparticles to algae, plants, and fungi, *Ecotoxicology*, 2008, **17**, 372–386.
50 X. Cao, R. Prozorov, Y. Koltypin, G. Katabi, A. Gedanken and J. Balogh, Synthesis of pure amorphous Fe_2O_3, *J. Mater. Res.*, 1997, **12**(2), 402–406.
51 P. S. Bassi, B. S. Randhawa and H. S. Jamwal, Mössbauer study of the thermal decomposition of iron(III) citrate pentahydrate, *J. Therm. Anal.*, 1984, **29**, 439–444, DOI: **10.1007/BF01913454**.
52 M. Gracheva, Z. Klencsár and Z. Homonnay, Revealing the nuclearity of iron citrate complexes at biologically relevant conditions, *BioMetals*, 2024, **37**, 461–475, DOI: **10.1007/s10534-023-00562-1**.